Semiconductor qubits based on fluorine implanted ZnMgSe/ZnSe quantum-well nanostructures

Y. M. Kim,[1,*] D. Sleiter,[2] K. Sanaka,[2,3] Y. Yamamoto,[2,3] J. Meijer,[4] K. Lischka,[1] and A. Pawlis[1,2,†]

[1]*Department Physik, Universität Paderborn, Warburger Straße 100, D-33098 Paderborn, Germany*

[2]*Edward L. Ginzton Laboratory, Stanford University, Stanford, California 94305-4088, USA*

[3]*National Institute of Informatics, 2-1-2 Hitotsubashi, Chiyoda-ku, Tokyo 101-8430, Japan*

[4]*RUBION, Ruhr Universität Bochum, Universitätsstraße 150, D-44780 Bochum, Germany*

(Received 12 October 2011; revised manuscript received 16 December 2011; published 6 February 2012)

It has been shown that the excitons bound to individual donors in epitaxially grown ZnMgSe/ZnSe quantum-well (QW) nanostructures provide suitable single-photon sources and optically controllable qubits for quantum information technology. Here we demonstrate ion implantation as an alternative fluorine doping method for ZnMgSe/ZnSe QWs. Photoluminescence measurements of F-implanted ZnSe QWs show the correlation between the number of sharp recombination peaks of F-donor bound excitons and the implantation dose as well as the saturation of the luminescence intensity related to a donor. The magnetospectroscopy results confirm the presence of two doubly connected Λ systems in the same way as for epitaxially grown and F-doped ZnSe QWs. If special techniques such as selective implantation through a mask and registration of single-ion impacts are applied on micro- and nanocavities, the ion implantation can be an attractive alternative fluorine doping method for quantum information technology based on fluorine impurities in ZnSe.

DOI: 10.1103/PhysRevB.85.085302 PACS number(s): 78.55.Et

I. INTRODUCTION

Various schemes of quantum information processing rely on a large number of independent stationary qubits (i.e., electron spins) and triggered single-photon sources.[1–4] These devices must demonstrate homogeneity and scalability in order to meet the current demands required for robust quantum computing and networking with high fidelity.[5,6] The homogeneity, which refers to the ability to generate coupling of stationary qubits (i.e., spins) through single photons that are equal in wavelength and in polarization, is certainly available in trapped atoms[7] and ions.[8–10] But the scalability, which refers to the engineering difficulty, remains challenging for this system, largely due to the elements of laser cooling and trapping. On the other hand, solid-state-based systems pose a reverse challenge. Solid-state devices can be more readily engineered, but finding the right materials in which many independent yet identical single photons are effectively generated is challenging. For instance, semiconductor quantum dots (QDs) can provide artificial atoms that can be readily implemented.[11,12] However, the homogeneity of single-photon sources and qubits based on epitaxially grown QDs is limited due to their natural size distribution.

Alternatively, impurities such as donor[13] or isoelectric centers[14] in semiconductors may bridge the gap between real and artificial atoms, since they provide identical atomic properties and can be easily integrated in semiconductors by epitaxial doping or by ion implantation. The electron bound to a single fluorine donor in ZnSe quantum wells (QWs) can be engineered as a physical qubit within an external magnetic field.[15] Due to the discrete nature of the QWs, the emission wavelength of an exciton bound to a neutral fluorine donor in the QW is well defined, and the line width remains relatively small. Besides the homogeneity, due to the 100% natural abundance of the spin-1/2 state in the ^{19}F nucleus, the F:ZnSe system may provide long-lived matter qubits as well. Moreover, unlike III-V based systems, isotopic purification[16] of the ZnSe host matrix to nuclear-spin-0 background can be achieved and might further reduce the nuclear decoherence of the electron spin. Silicon-based systems can overcome the nuclear decoherence,[17–19] but due to the indirect band gap of silicon they are optically dark. Furthermore, the availability of micro- and nanofabrication technologies for ZnSe[20] may offer enough scalability to generate large arrays of coupled qubits in quantum networks. We have recently demonstrated the quantum interference between indistinguishable single photons generated by the radiative decay processes of excitons bound to isolated fluorine impurities in ZnMgSe/ZnSe quantum-well (QW) nanostructures.[21] Also, the presence of optically controllable electron spins in a bound state to a donor in ZnSe has been demonstrated by magnetospectroscopy.[15] These results were obtained from molecular beam epitaxy (MBE) grown ZnMgSe/ZnSe QWs, which were delta-doped with fluorine donors during growth (in the following referred to as "expitaxially doped" QWs).

Here, we demonstrate an alternative fluorine doping method via ion implantation. Previously, fluorine doping has been achieved by epitaxial doping with a ZnF_2 cracker cell. Although the cracker cell provides sufficient thermal energy for dissociating ^{19}F atoms from ZnF_2 molecules, there is the possibility of a small fraction of fluorine atoms to be embedded in ZnSe as ZnF or as ZnF_2 complexes. The ion-implantation method allows for pure selection of ^{19}F ions by mass separation. Consequently, the probability of forming other zinc-fluorine complexes in the sample is minimized. Furthermore, precise control of the doping concentration is possible by modulating the implantation dose by the ion current in a wide range between 10^{10} and 10^{13} cm^{-2}. Also, a localized doping technique is available by selective implantation through a several nanometer sized mask or Atomic Force Microscope (AFM) tip, which would otherwise be extremely difficult in the purely epitaxial processes.[22,23] Moreover, the possibility of implanting countable single ions on a nanometer scale has been shown for highly charged $^{31}P^{2+}$ ions[24] or by using ion traps.[25,26] The possibility of registering single fluorine impurities in ZnSe microcavities would enable the F:ZnSe

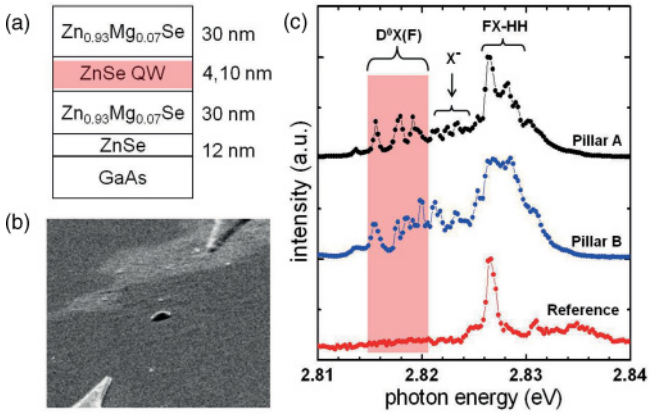

FIG. 1. (Color online) Sample structure and μ-PL spectra. (a) Schematic of the sample structure; the striped region (red) is where most of the implanted fluorine is distributed. (b) Scanning-electron image of a 200-nm-diameter nanopillar with its markers. (c) PL spectra of two nanopillars and a reference PL spectrum measured at 5 K. The FX-HH region represents the heavy-hole free-exciton emission, and the X^- region indicates the charged free-exciton complex. The region denoted by $D^0X(F)$ corresponds to the radiative recombination of excitons bound to isolated fluorine donors.

system to be connected with ZnSe-based optical waveguides for integrated optical qubit coupling. Although low doping of fluorine could be achieved for micro- and nanocavities with purely epitaxial processes, the residual fluorine impurities in the waveguide region may hinder the clear transfer of photons. The undoped ZnSe host matrix can be prepared using MBE. The structuring of microcavities, nanocavities, and waveguides can be accomplished via optical and *e*-beam lithography and via wet-chemical etching techniques. Then the single fluorine impurities can be implanted in the micro- and nanocavities selectively, keeping the fluorine level in the waveguide region down to the background level.

II. EXPERIMENT

The ZnMgSe/ZnSe quantum-well (QW) structures were grown with MBE. A typical sample structure is shown in Fig. 1(a). First, a 12-nm-thick buffer layer of undoped ZnSe is deposited on GaAs-(001) substrates for clean interface properties. The 4- and 10-nm ZnSe QWs are buried between two 30-nm-thick ZnMgSe cladding layers with an estimated magnesium content of about 5–10%. The fluorine doping is achieved by ion implantation, and a subsequent annealing of the MBE grown samples is performed at 400 °C for 30 s to reduce the implantation damage. Principally, the annealing of the implanted sample may cause a degradation effect upon the quantum-well interfaces. However, we have not observed any notable shift of the luminescence in our ZnSe QW due to the annealing process with the given parameter. An acceleration voltage of 24 kV was chosen by simulating the distribution of ions in the sample such that the linear concentration reaches a maximum in the QW region. The implantation dose was varied between 10^{10} and 10^{13} cm^{-2} with a linear concentration of 0.15 pm^{-1}. After the implantation, nanopillars 200 nm in diameter and coordinating markers were fabricated through electron-beam writing and wet-chemical etching techniques. A scanning electron micrograph of a typical structure is shown in Fig. 1(b). The number of implanted ions in the nanopillars is estimated by the implantation dose. For instance, a fluorine implantation dose of 1×10^{11} cm^{-2} applied to the sample results in an average amount of 2 F donors that are distributed in the 4-nm-thick ZnSe QW region of a nanopillar with 200 nm diameter. The microphotoluminescence (μ-PL) of the nanostructures was above-band excited with a solid-state laser system at a wavelength of 377 nm. A spectrometer with 150 mm focal length was used to collect the μ-PL light emission at 5 K with a resolution limit of 0.6 meV (0.1 nm). For magneto-PL measurement, a 408-nm GaN laser-diode was chosen. The μ-PL spectrum was collected through a spectrometer (750 mm focal length) with a liquid-N_2-cooled charge-coupled-device camera with a resolution limit of 0.13–0.2 meV (0.02–0.03 nm).

III. RESULTS AND DISCUSSION

Figure 1(c) shows three μ-PL spectra. Pillars A and B are the PL spectra from two different nanopillars of the same wafer. The reference μ-PL spectrum is from a pillar in a different wafer where the implantation dose is 5×10^{10} cm^{-2} with about 0–1 donors in the pillar. The implantation dose for both pillars A and B is 5×10^{11} cm^{-2} where 10 F donors are estimated to be present in a nanopillar with 200 nm diameter. In all μ-PL spectra, three primary spectral regions with various sharp PL peaks can be distinguished. The highest-energy emission region of the spectra in Fig. 1(c), labeled FX-HH around 2.827 eV, is the heavy-hole free-exciton emission. The second region, denoted by X^-, corresponds to the trion state or the charged free-exciton complex that is often observed in II-VI semiconductor QWs.[27] The third region, marked by $D^0X(F)$, indicates the radiative recombination of excitons bound to isolated fluorine donors. In the reference PL, there is no notable PL emission from the $D^0X(F)$ region. In the PL spectrum from pillar A, there are several notable peaks observed in the $D^0X(F)$ region at 2.816, 2.818, and 2.819 eV. We identify these peaks as F-donor bound-exciton emission lines. A typical line width of these peaks is 0.6 ± 0.1 meV, as limited by the resolution of our spectrometer. According to the previous results presented in Ref. 21, the homogeneous line width of the bound-exciton recombination is 50–100 μeV. It indicates that, in our spectra, more than one F donor may contribute to each of the emission lines. The energy difference between the FX-HH and $D^0X(F)$ transitions reveals the binding energy of the bound excitons. In pillar A, this energy is between 7 and 10 meV, which is in good agreement with previously investigated expitaxially doped ZnSe QWs.[28] The separation of $D^0X(F)$ peaks in device A (1.5–2 meV) can be explained by monolayer fluctuations in the QW width. The fluorine donors are statistically distributed through the cross section of the QW, which may cause a variation of confinement energy due to their locations within the QW. This may lead to a broadening of the emission lines which, at least within the resolution limit of our spectrometer, is not observed. Thus the energy separation of $D^0X(F)$ related emission lines is due to the monolayer fluctuation in the QW. The observed separation of about 2 meV is in good agreement with the calculated value of 1.8 meV for one-monolayer steps. In pillars A and B in

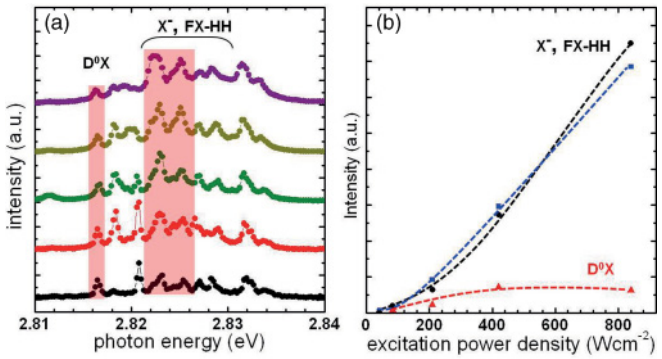

FIG. 2. (Color online) (a) Power-dependent PL spectra of F-implanted ZnSe QWs at 5 K. As the excitation power density increases, donor-bound exciton emission lines are saturated while those of the analyzed X^- and FX increase continually. (b) Integrated peak intensity of the selected $D^0X(F)$ line and that of the selected X^-, FX in (a).

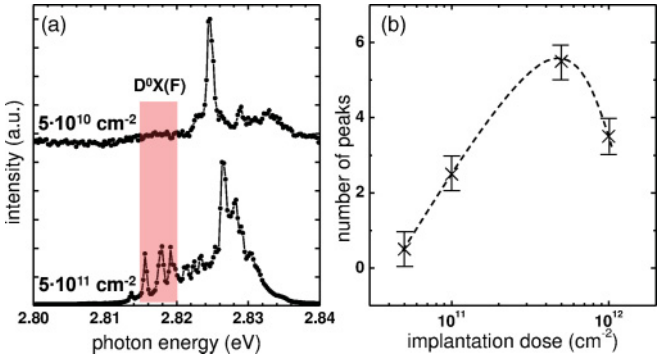

FIG. 3. (Color online) Quantity of $D^0X(F)$ peaks versus the implantation dose. (a) μ-PL spectra from two nano pillars with different implantation doses. A clear increase of the number of peaks is seen in the $D^0X(F)$ region. (b) Average number of $D^0X(F)$ peaks as a function of implantation dose. The quantity of $D^0X(F)$ peaks is proportional to implantation doses lower than 5×10^{11} cm^{-2}.

Fig. 1(c), the same peak in the $D^0X(F)$ at 2.8158 eV is seen in both PL spectra deviated within the resolution limit of our spectrometer. Regardless of the energy separation caused by the monolayer fluctuation, statistical matching of the emission energy among some of the $D^0X(F)$ peaks is observed.

Figure 2 shows the PL spectra from a nanopillar measured at 5 K with increasing excitation power density. In Fig. 2(a), μ-PL intensities of all three spectral regions are compiled with increasing excitation power densities. In Fig. 2(b) the intensity of the selected $D^0X(F)$ peak at 2.8162 eV and two main peaks at 2.8230 and 2.8251 in the X^- and FX-HH regions are quantified as a function of different excitation power densities. At excitation powers lower than 400 W cm^{-2}, the μ-PL intensity of the $D^0X(F)$ peak at 2.8162 eV increases proportionally with the excitation power density. At excitation powers higher than 400 W cm^{-2} the indicated peak at 2.8162 eV is saturated, while the intensity of the two main peaks in the X^- and FX-HH regions show a superlinear increase with increasing excitation power. Such a result clearly indicates the presence of bound-exciton states in the QW.

Figure 3(a) shows the μ-PL spectra from two nanopillars with different F-implantation doses of 5×10^{10} and 5×10^{11} cm^{-2}, where about 1 and 10 F donors, respectively, are statistically distributed in the QW. In most of the 200-nm nanopillars we have not observed any peak in the $D^0X(F)$ region for a dose of 5×10^{10} cm^{-2}. Since not all implanted fluorine ions are expected to be rightly incorporated as active donors, it shows that the F-implantation dose was too low to observe $D^0X(F)$ peaks. With one-magnitude higher dose, where about 10 F donors could be present, 5–6 sharp $D^0X(F)$ PL peaks are observed. As discussed previously, the monolayer fluctuation of QWs causes the emission energies to be separated by 1.5–2 meV. Figure 3(b) shows the correlation between the average number of $D^0X(F)$ peaks with increasing implantation dose. For implantation doses lower than 5×10^{11} cm^{-2} the quantity of $D^0X(F)$ peaks is correlated with the increasing implantation dose. The result clearly demonstrates the ability to introduce F as donors via the implantation doping method. The decrease in the number of $D^0X(F)$ peaks with the highest implantation dose in Fig. 3(b) suggests that a multiple of donors could have contributed to the emission at the same energy, as the number of donors exceeds the number of QW fluctuation levels. Also, there may be an upper limit of the implantation dose, above which the implantation damage was not completely removed by the annealing procedure.

The relevant transitions and energy spectra related to the $D^0X(F)$ are shown in Figs. 4(a) and 4(b) (for a review on magnetospectroscopy, see also Refs. 29–31). Because of the compressive strain in the whole structure, the degeneracy between the heavy and light hole states in the ZnSe QW is lifted,[13,28] where the HH band provides the lowest-energy hole states. The Voigt-geometry data in Fig. 4(b) show a fourfold split with linear polarization, which is consistent with F-donor bound-exciton emission. From the measured line splits, we infer an electron g factor of $g_e = 1.1(\pm 0.2)$, which is in good agreement with the value of $g_e = 1.2$ previously measured on epitaxially doped F:ZnSe QWs.[15] The heavy holes in the bound-exciton complex are weakly coupled to the magnetic field, leading to an in-plane heavy-hole g factor $|3g_{hh}^{\perp}| = 0.0(\pm 0.2)$ for a 10-nm QW and $|3g_{hh}^{\perp}| = 0.1(\pm 0.2)$ for a 4-nm QW. The Voigt data clearly demonstrate that, via the ion-implantation doping method, the presence of two doubly connected Λ systems is established in the same way as with epitaxially F-doped samples, which makes the F donor suitable for several proposed quantum information technology schemes. In Faraday geometry [see Fig. 4(b)], a twofold split of the magneto-PL is observed. From the measured line split, we infer a difference in the out-of-plane heavy-hole and electron g factors, $|3g_{hh}^{||} - g_e| = 0.5(\pm 0.2)$ for a 10-nm QW and $|3g_{hh}^{||} - g_e| = 0.8(\pm 0.2)$ for a 4-nm QW. The measured values in both Voigt and Faraday geometries are consistent with previously measured magneto-PL results of a 3-nm F:ZnSe QW with epitaxial doping.[15]

IV. CONCLUSIONS

In conclusion, we introduced ion implantation as an alternative fluorine doping method for ZnMgSe/ZnSe QW structures.

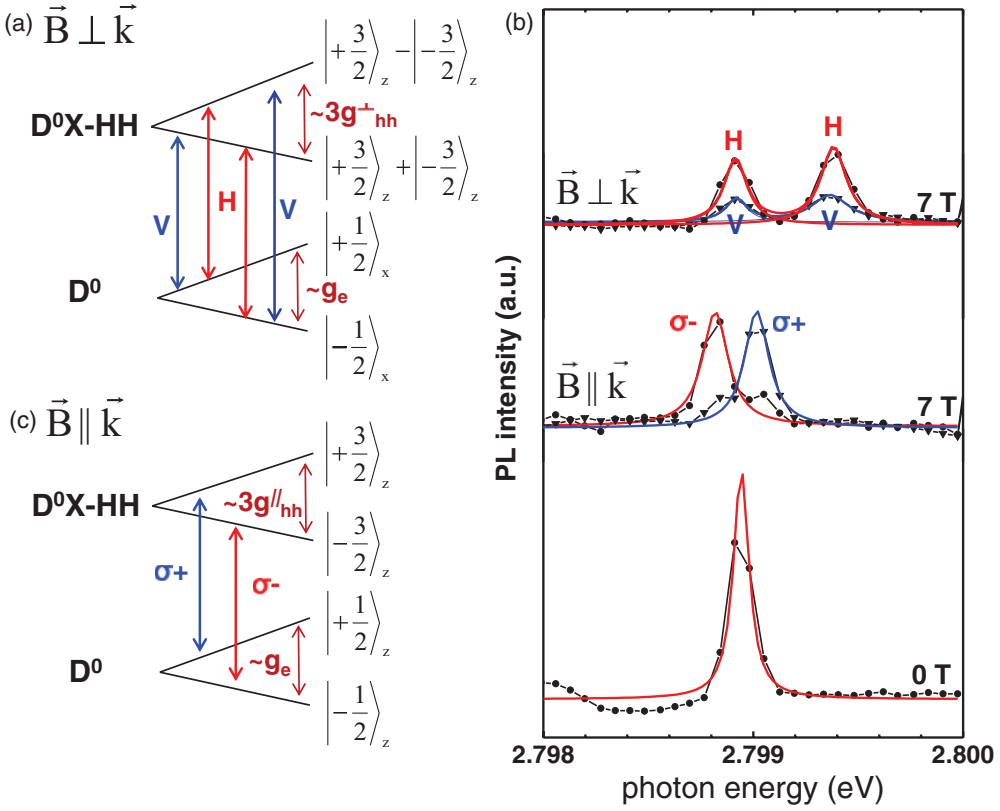

FIG. 4. (Color online) Magneto-PL data for 200-nm-diameter mesas of a 10-nm F-doped ZnSe QW measured at 5 K. (a) Energy spectrum in Voigt geometry (bound exciton D^0X; bound electron D^0; heavy hole HH). (b) PL at 0 T and with applied magnetic field of 7 T in Voigt and Faraday geometries. (c) Energy spectrum in Faraday geometry.

Photoluminescence measurements show a correlation between the number of sharp recombination peaks of F-donor bound excitons and the implantation dose as well as the saturation of the luminescence intensity related to a bound state. The consistent magneto-PL data in both Faraday and Voigt geometries with previously investigated epitaxially doped F:ZnSe indicate that, via ion-implantation method, the presence of optically controllable electron spins of neutral donors in ZnSe can be established. With the additional advantages that the ion-implantation doping method can provide, such as the selective implantation through a mask and the possibility of registering single ion impacts on micro- and nanocavities for optical coupling with waveguides, ion-implantation presents itself as an attractive alternative doping method for quantum information technology based on fluorine impurities in ZnSe.

ACKNOWLEDGMENTS

This work was supported by NICT, MEXT, NIST (Grant No. 60NANB9D9170), NSF (Grant No. CCR-08 29694), University of Tokyo Special Coordination Funds for Promoting Science and Technology, NTT Basic Research Laboratories, and by the Japan Society for the Promotion of Science (JSPS) through its Funding Program for World-Leading Innovative R&D on Science and Technology (FIRST). We further acknowledge the financial support of the DFG Graduiertenkolleg GRK-1464.

*ymkim@mail.upb.de
†apawlis@mail.upb.de

[1] I. L. Chuang and Y. Yamamoto, Phys. Rev. A **52**, 3489 (1995).
[2] E. Knill, R. Laflamme, and G. J. Milburn, Nature (London) **409**, 46 (2001).
[3] X. L. Feng, Z. M. Zhang, X. D. Li, S. Q. Gong, and Z. Z. Xu, Phys. Rev. Lett. **90**, 217902 (2003).
[4] J. I. Cirac, P. Zoller, H. J. Kimble, and H. Mabuchi, Phys. Rev. Lett. **78**, 3221 (1997).
[5] D. P. DiVincenzo, Fortschr. Phys. **48**, 771 (2000).
[6] T. D. Ladd, F. Jelezko, R. Laflamme, Y. Nakamura, C. Monroe, and J. L. O'Brian, Nature **464**, 45 (2010); L. M. Duan, M. D. Lukin, J. I. Cirac, and P. Zoller, Nature (London) **414**, 413 (2001).
[7] J. Beugnon, M. P. A. Jones, J. Dingjan, B. Darquie, G. Messin, A. Browaeys, and P. Grangier, Nature (London) **440**, 779 (2006).
[8] S. Seidelin, J. Chiaverini, R. Reichle, J. J. Bollinger, D. Leibfried, J. Britton, J. H. Wesenberg, R. B. Blakestad, R. J. Epstein, D. B.

Hume, W. M. Itano, J. D. Jost, C. Langer, R. Ozeri, N. Shiga, and D. J. Wineland, Phys. Rev. Lett. **96**, 253003 (2006).

[9]P. Maunz, D. L. Moehring, S. Olmschenk, K. C. Younge, D. N. Matsukevich, and C. Monroe, Nature Phys. **3**, 538 (2007).

[10]S. Olmschenk, D. N. Matsukevich, P. Maunz, D. Hayes, L. M. Duan, and C. Monroe, Science **323**, 486 (2009).

[11]R. B. Patel, A. J. Bennett, I. Farrer, C. A. Nicoll, D. A. Ritchie, and A. J. Shields, Nature Photonics **4**, 632 (2010).

[12]E. B. Flagg, A. Muller, S. V. Polyakov, A. Ling, A. Migdall, and G. S. Solomon, Phys. Rev. Lett. **104**, 137401 (2010).

[13]A. Pawlis, K. Sanaka, S. Götzinger, Y. Yamamoto, and K. Lischka, Semicond. Sci. Tech. **21**, 1412 (2006).

[14]A. Muller, P. Bianucci, C. Piermarocchi, M. Fornari, I. C. Robin, R. André, and C. K. Shih, Phys. Rev. B **73**, 081306(R) (2006).

[15]K. D. Greve, S. M. Clark, D. Sleiter, K. Sanaka, T. D. Ladd, M. Panfilova, A. Pawlis, K. Lischka, and Y. Yamamoto, Appl. Phys. Lett. **97**, 241913 (2010).

[16]R. Lauck and E. Schnherr, J. Cryst. Growth **197**, 513 (1999).

[17]A. M. Tyryshkin, S. A. Lyon, A. V. Astashkin, and A. M. Raitsimring, Phys. Rev. B **68**, 193207 (2003).

[18]S. D. Sarma, R. de Sousab, X. Huc, and B. Koillerd, Solid State Commun. **133**, 737 (2005).

[19]A. Yang, M. Steger, D. Karaiskaj, M. L. W. Thewalt, M. Cardona, K. M. Itoh, H. Riemann, N. V. Abrosimov, M. F. Churbanov, A. V. Gusev, A. D. Bulanov, A. K. Kaliteevskii, O. N. Godisov, P. Becker, H.-J. Pohl, J. W. Ager, III, and E. E. Haller, Phys. Rev. Lett. **97**, 227401 (2006).

[20]M. Panfilova, A. Pawlis, C. Arens, S. M. de Vasconcellos, G. Berth, K. P. Hsch, V. Wiedemeier, A. Zrenner, and K. Lischka, Microelectron. J. **40**, 215 (2009).

[21]K. Sanaka, A. Pawlis, T. D. Ladd, K. Lischka, and Y. Yamamoto, Phys. Rev. Lett. **103**, 053601 (2009).

[22]J. Meijer, S. Pezzagna, T. Vogel, B. Burchard, H. H. Bukow, I. W. Rangelow, Y. Sarov, H. Wiggers, I. Plümel, F. Jelezko, J. wrachtrup, F. Schmidt-Kaler, W. Schnitzler, and K. Singer, Appl. Phys. A **91**, 567 (2008).

[23]S. Pezzagna, D. Wildanger, P. Mazarov, A. D. Wieck, Y. Sarov, I. Rangeow, B. Naydenov, F. Jelezko, S. W. Hell, and J. Meijer, Small **6**, 2117 (2010).

[24]T. Schenkel, A. Persaud, S. J. Park, J. Meijer, J. R. Kingsley, J. W. McDonald, J. P. Holder, J. Bokor, and D. H. Schneider, J. Vac. Sci. Technol. B **20**, 2819 (2002).

[25]J. Meijer, T. Vogel, B. Burchard, I. W. Rangelow, L. Bischoff, J. Wrachtrup, M. Domhan, F. Jelezko, W. Schnitzler, S. A. Schulz, K. Singer, and F. Schmidt-Kaler, Appl. Phys. A **83**, 321 (2006).

[26]W. Schnitzler, N. M. Linke, R. Fickler, J. Meijer, F. Schmidt-Kaler, and K. Singer, Phys. Rev. Lett. **102**, 070501 (2009).

[27]G. V. Astakhov, D. R. Yakovlev, V. P. Kochereshko, W. Ossau, J. Nürnberger, W. Faschinger, and G. Landwehr, Phys. Rev. B **60**, R8485 (1999).

[28]A. Pawlis, M. Panfilova, D. J. As, K. Lischka, K. Sanaka, T. D. Ladd, and Y. Yamamoto, Phys. Rev. B **77**, 153304 (2008).

[29]J. L. Merz, H. Kukimoto, K. Nassau, and J. W. Shiever, Phys. Rev. B **6**, 545 (1972).

[30]P. J. Dean, D. Bimberg, and F. Mansfield, Phys. Rev. B **15**, 3906 (1977).

[31]V. A. Karasyuk, D. G. S. Beckett, M. K. Nissen, A. Villemaire, T. W. Steiner, and M. L. W. Thewalt, Phys. Rev. B **49**, 16381 (1994).